30. Dresel SHJ, Kung M-P, Plössl K, Meegalla SK, Kung HF. Pharmacological effects of dopaminergic drugs on in vivo binding of [^{99m}Tc]TRODAT-1 to the central dopamine transporters in rats. *Eur J Nucl Med* 1998;25:31–39.
31. Morisette M, Di Paolo T. Sex and estrous cycle variations of rat striatal dopamine uptake sites. *Neuroendocrinology* 1993;58:16–22.
32. Morisette M, Biron D, Di Paolo T. Effect of estradiol and progesterone on rat striatal dopamine uptake sites. *Brain Res Bull* 1990;25:49–422.
33. Morisette M, Di Paolo T. Effects of chronic estradiol and progesterone treatments of ovariectomized rats on brain dopamine uptake sites. *J Neurochem* 1993;60:1876–1883.
34. Ichise M, Ballinger JR, Vines D, Tsai S, Kung HF. Simplified quantification and reproducibility studies of dopamine D2-receptor binding with iodine-123-IBF SPECT in healthy subjects. *J Nucl Med* 1997;38:31–37.
35. Seibyl JP, Laruelle M, van Dyck CH, et al. Reproducibility of iodine-123-β-CIT SPECT brain measurement of dopamine transporters. *J Nucl Med* 1996;37:222–228.
36. Tiihonen J, Kuikka J, Bergström K, Lepola U, Koponen H, Leinonen E. Dopamine reuptake sites densities in patients with social phobia. *Am J Psychiatry* 1997;154:239–242.
37. Habraken JBA, Booij J, van Royen EA, Slomka PJ. Quantification of the functional dopaminergic system using an automatic algorithm [Abstract]. *J Nucl Med* 1997;38:60.

Fluorine-18-Fluoro-L-DOPA Dosimetry with Carbidopa Pretreatment

W. Douglas Brown, Terrence R. Oakes, Onofre T. DeJesus, Michael D. Taylor, Andrew D. Roberts, Robert J. Nickles and James E. Holden

Departments of Radiology and Medical Physics, University of Wisconsin–Madison Medical School, Madison, Wisconsin

This article presents dosimetry based on the measurement of fluoro-DOPA activity in major tissues and in the bladder contents in humans after oral pretreatment with 100 mg carbidopa. **Methods:** Bladder activity was measured continuously by external probe and calibrated using complete urine collections. Quantitative dynamic PET scans provided time-activity curves for the major organs. Bladder wall dosimetry was calculated using the methods of *MIRD Pamphlet No. 14*. Effective dose was calculated as described in *ICRP Publication 60*. **Results:** Mean absorbed dose to the bladder wall surface per unit administered activity was 0.150 mGy/MBq (0.556 rad/mCi) with the realistic void schedule used in our studies. The dose was 0.027 mGy/MBq (0.101 rad/mCi) to the kidneys, 0.0197 mGy/MBq (0.0728 rad/mCi) to the pancreas, and 0.0186 mGy/MBq (0.0688 rad/mCi) to the uterus. Absorbed doses to other organs were an order of magnitude or more lower than the bladder, 0.009–0.015 mGy/MBq. The effective dose per unit administered activity was 0.0199 mSv/MBq (0.0735 rem/mCi.) **Conclusion:** Urinary excretion of fluoro-DOPA was altered significantly by pretreatment with carbidopa. In general, any manipulation of tracer metabolism in the body should be expected to produce changes in biodistribution and dosimetry. The largest radiation dose was to the bladder wall, for which our estimate was one-fifth of that from the original report. The methods used reflect realistic urinary physiology and typical use of this tracer. The principles of *MIRD Pamphlet No. 14* should be used in planning studies using tracers excreted in the urine to minimize the absorbed dose.

Key Words: fluorine-18-DOPA; fluoro-DOPA PET; bladder dosimetry; medical internal radiation dose

J Nucl Med 1998; 39:1884–1891

The original published dosimetry for [^{18}F]−6-fluoro-L-3,4-dihydroxy-phenylalanine (^{18}F-DOPA, fluoro-DOPA) dates from 1985 (*1*), very early in the use of this tracer for PET imaging of brain dopaminergic systems (*2*). Viewed from more than a decade later, this foundation work has several limitations. First, in the absence of continuous bladder activity data the authors chose to base their calculations on the assumption that all the activity that appeared in the bladder by approximately 4 hr after injection was present instantaneously at the time of the injection. In addition, a relatively large postvoid urine residual value was used (20%.) These calculations, therefore, intentionally represented a very conservative *upper limit* estimate of bladder wall absorbed dose. Second, differential tissue activity estimates are based on data from two dogs, with no corroborating human evidence. Third, these measurements were made before the institution of oral carbidopa pretreatment, which is now a universal adjunct to ^{18}F-DOPA PET imaging (*3–6*). This drug blocks peripheral aromatic L-amino acid decarboxylase (AAAD); its administration markedly improves imaging by preventing the early decarboxylation of ^{18}F-DOPA to ^{18}F-dopamine outside the brain. Since this also causes changes in the time course of ^{18}F-DOPA metabolism and the relative amounts of the various labeled metabolites, the use of carbidopa has an effect on renal excretion and, therefore, on dosimetry for the bladder and other organs. Fourth, the original dosimetry calculations were based on the International Commission on Radiological Protection (ICRP) *Standard Man* model, which has a static urinary bladder. Over the last two decades methods have been developed for more accurate estimation of absorbed dose from bladder contents, leading to the revision of bladder dose calculations published in *MIRD Pamphlet No. 14* from the Medical Internal Radiation Dose (MIRD) Committee of the Society of Nuclear Medicine (*7*). Two published articles (*8–9*), a doctoral thesis (*10*) and two abstracts (*11–12*) in recent years have addressed some, but not all, of these concerns.

The original published data demonstrated that the upper limit of absorbed dose from ^{18}F-DOPA administration was within a tolerable range for human use, but more accurate human absorbed dose estimates are needed for several reasons. First, modern targets (*13*) and syntheses (*14*) have made it possible to produce fluoro-DOPA in amounts not readily obtainable in earlier years; radiation dosimetry has, therefore, become the limiting factor in the dose administered. Second, initial dosimetry estimates allow only small administered doses of fluoro-DOPA (*9,12*), leading to severely count-limited studies. Such noisy data have limited sensitivity to the changes brought about by disease and limit the ability to correlate PET data with clinical parameters of disease progression. Third, as PET evaluations of the nigrostriatal system have progressed and more tracers have become available, it is more common for an experiment to require multiple tracer injections. Many pharmacologic or pathophysiologic experiments require the administration of ^{18}F-DOPA on two or more occasions, or its use in conjunction with markers of dopamine postsynaptic receptors

Received Jun. 6, 1997; revision accepted Feb. 12, 1998.
For correspondence or reprints contact: W. Douglas Brown, MD, Department of Radiology, E3/311 CSC, 600 Highland Ave., Madison, WI 53792-3252.

(*15,16*), dopamine presynaptic reuptake sites (*17*), brain glucose utilization (*16,18*) or other aspects of neuronal function. The bladder wall is the critical organ for many of these tracers. Fourth, as use of this tracer becomes more common, an accurate understanding of ^{18}F-DOPA dosimetry becomes increasingly important for devising strategies for minimizing the absorbed dose. In particular, dosimetry calculations based on a physiologically realistic bladder model (*7,19*) may be used with accurate urinary excretion data in planning aspects of the experimental procedure such as subject hydration and scan timing. Fifth, the increasingly frequent use of the *effective dose* (*20*) as a means of characterizing the biologic significance of a radiation dose—its use being often encouraged by radioactive drug research committees and institutional review boards—points to the need for an accurate published value for ^{18}F-DOPA. Finally, accurate dosimetry is needed as this tracer moves toward eventual clinical use as well as inclusion in *USP Dispensing Information*.

MATERIALS AND METHODS

Patients

Informed consent was obtained from all subjects. All protocols had the approval of our Human Subjects and Radioactive Drug Research Committees. The majority of the information needed for fluoro-DOPA dosimetry was collected concurrent with dynamic imaging of the brain, during several studies of striatal dopaminergic function in healthy control subjects and in parkinsonian patients. Measurements of bladder contents and whole-body rectilinear scans were attempted in 23 consecutive subjects, both parkinsonian and healthy. Because of technical failures and the limitations of some of our elderly and ill subjects, complete urinary measurements were obtained in 18 of these subjects and rectilinear scans in 19. Quantitative dynamic whole-body imaging was performed on two additional subjects. Dynamic blood samples from 34 subjects were used to assess the time course of total radioactivity in the plasma and whole blood. Finally, dynamic brain scans from 11 subjects with normal fluoro-DOPA uptake (10 healthy control subjects and one subject with a nonparkinsonian tremor) were included to assess the time course of activity in various brain tissues.

Urine Measurements

Bladder contents time-activity curves were measured during routine brain imaging as follows. Each subject was given 100 mg carbidopa orally 1 hr before tracer injection and asked to empty the bladder completely before entering the PET scanner; the time of this void was recorded. The subject was placed on the PET scanner couch in a comfortable supine position with the striata centered in the scanner field of view, and a 20-min transmission scan was obtained. A 1-inch heavily collimated sodium iodide probe was positioned such that the crystal was 3-to-6 in. above the anterior surface of the pelvis, centered just above the pubic ramus. In this position, the entire volume of the bladder was expected to be within the field of view of the detection device. This probe was interfaced to a counting card in a personal computer.

A tracer dose of 63–285 MBq (1.7–7.7 mCi) ^{18}F-DOPA (specific activity approximately 0.6 mCi/μmol) was injected intravenously and bladder activity was monitored continuously for 90–110 min; counts were stored every 6 sec. At the completion of brain imaging, the probe was placed over the upper abdomen and over the upper thigh for 30 sec each to measure background activity. The subject then was asked to void, and the complete urine sample was collected; void time, volume and activity were recorded. The subject was returned to the scanning couch as quickly as possible, and the probe was repositioned over the bladder as described above. A 1-min postvoid bladder activity measurement was obtained. In six subjects, a second complete urine sample was collected at between 2 and 3 hr after injection.

The voided volume and time between voids were used to determine the mean urine production rate. The measured bladder counts were calibrated by considering the total voided activity to be equal to the difference between the bladder probe counting rates before voiding and after voiding. Background subtraction was then applied to yield the bladder contents time-activity curve. The fraction of administered tracer remaining in the tissues of the body as a function of time was obtained by correcting the calibrated bladder curve for physical decay and dividing by the administered dose, then subtracting this curve from unity.

Whole-Body PET

Early studies included in this article were performed on a CTI 933/04 scanner (CTI, Knoxville, TN) with the capability of performing moving-bed, rectilinear body scans. These provided nonquantitative images for visual interpretation of activity distribution. Preliminary results from these scans were previously reported (*11*). Rectilinear scans were performed immediately after the first postinjection void, typically beginning 100–130 min after injection and, therefore, depicted the whole-body distribution of activity at approximately 2 hr after injection. It was anticipated that any specific accumulation of tracer in any large organ would be visible on these scans.

More recently, using a GE Advance PET imaging device (GE Medical Systems, Waukesha, WI), quantitative whole-body dynamic scans were performed as follows. One hundred milligrams carbidopa were administered orally 1 hr before tracer injection. Each subject was positioned comfortably on the scanner bed, using straps to support the arms in a neutral position and minimize motion. Transmission scans were obtained over five contiguous 15-cm segments from the base of the head to approximately the middle of the thigh; transmission scan duration was 6 min per position. The scanner then was programmed to acquire a 27-frame dynamic scan with specified bed movements between frames, such that four to eight frames were obtained for each of the five body segments over the next 97 min.

Using the corresponding transmission scans, the dynamic frames were reconstructed individually with measured attenuation correction and without decay correction. The individual frames from each body segment were combined to yield five discontinuous dynamic scans. Any major organ that could be clearly identified on either the emission images or transmission images was selected for a manually drawn region of interest (ROI). Discontinuous curves of activity concentration versus time were generated from these ROIs for the major salivary glands, lungs, liver, spleen, pancreas, kidneys, red marrow (from the lumbosacral spine) and skeletal muscle. The skeletal muscle values were obtained as a mean from several ROIs that included muscles from the shoulder girdle, gluteal muscles and the quadriceps femoris.

Dynamic Brain PET

Because brain accumulation of fluoro-DOPA is diminished in parkinsonian patients, only nonparkinsonian subjects were used for brain dosimetry measurements. Of 11 such subjects in a study of brain dopamine metabolism, 8 had two scans each, for a total of 19 measurements. Both two-dimensional and three-dimensional mode acquisitions were performed. For dosimetry purposes, there was no systematic difference between the two-dimensional and three-dimensional scans, so they were considered together. Imaging was performed on a GE Advance PET instrument. Oral carbidopa was given 1 hr before tracer injection. The scanning protocol included a 20-min transmission scan followed by a 90-min dynamic emission study after injection of approximately 259 MBq (7 mCi)

fluoro-DOPA. The dynamic study consisted of 18 frames of increasing duration from initial 30-sec frames to final 10-min frames.

An automated thresholding method was used to identify the boundaries of individual caudate nuclei and putamina, as well as the surface of the brain. A manually drawn ROI was placed within the occipital lobe (striate cortex), an area of gray matter without specific fluoro-DOPA uptake that is often used for tissue-derived input functions for modeling of fluoro-DOPA uptake (*21*). Graphs of activity concentration versus time were generated from these ROIs.

Blood Samples

Arterial or venous blood sampling was performed in our several protocols for deriving metabolite data and activity input functions for brain fluoro-DOPA modeling. For purposes of dosimetry, there was no significant difference between arterial and venous blood samples, so these were handled together. Discrete 2–3 ml samples were obtained as rapidly as possible during the 2 min after tracer administration and, at progressively longer intervals thereafter, until 90 min after injection. Samples were immediately placed into ethylenediaminetetraacetic acid tubes and placed in an ice bath. Five hundred microliters of whole blood were pipetted from selected samples (5, 30, 60, 90 min). In four subjects, whole blood was pipetted from every sample. Each sample was centrifuged at 3000 rpm for 7 min, and 500 μl of the supernatant plasma was pipetted. Activity in the plasma and whole-blood samples was measured in a calibrated gamma counter and corrected for decay from the time of sampling.

General MIRD Schema Calculations

The schema developed by the Medical Internal Radiation Dosimetry (MIRD) Committee of the Society of Nuclear Medicine (*22–25*) provides simplifications and tabulations for use in radiation absorbed dose calculations. The general MIRD equation for mean absorbed dose $\bar{D}$ per unit administered activity A_0 is:

$$\frac{\bar{D}}{A_0} = \tau S \qquad \text{Eq. 1}$$

S is tabulated in *MIRD Pamphlet No. 11* (*24*). Residence time τ is the integral of the time-activity curve normalized to administered activity, or (equivalently) the time integral of the fraction of administered activity within an organ:

$$\tau = \int_0^\infty \frac{A(t)}{A_0}\,dt \qquad \text{Eq. 2}$$

In the current study, blood and tissue data were measured as activity concentrations. The activity concentration was divided by the administered activity to yield graphs of fractional activity per volume versus time for each tissue, and the results were averaged across subjects. The time integral of fractional activity per unit volume is the residence time per unit volume, τ/V. Numerical integration was used to calculate τ/V for each tissue during the data collection period.

After bolus injection of fluoro-DOPA, there is rapid equilibration in the tissues, such that only the tracer leaving an organ needs to be considered in detail. A sum of exponential components approximates this biological egress to a useful accuracy. Thus, biological outflow from an organ may be described by the sum of two exponential components with coefficients α_1 and α_2 and time constants λ_1 and λ_2. Activity as a function of time is given by:

$$A(t)/A_0 = \alpha_1 e^{-(\lambda_1+\lambda_p)t} + \alpha_2 e^{-(\lambda_2+\lambda_p)t} \qquad \text{Eq. 3}$$

where A_0 is the activity at time = 0 and λ_p is the physical decay constant for the nuclide. Integration of Equation 3 yields:

$$\int_t^\infty \frac{A(t)}{A_0}\,dt = \frac{\alpha_1}{\lambda_1 + \lambda_p} + \frac{\alpha_2}{\lambda_2 + \lambda_p} \qquad \text{Eq. 4}$$

The integral from time t to infinity also may be written:

$$\int_t^\infty \frac{A(t)}{A_0}\,dt = \frac{\alpha_1}{\lambda_1 + \lambda_p} + \frac{\alpha_2}{\lambda_2 + \lambda_p} - \int_0^t \frac{A(t)}{A_0}\,dt \qquad \text{Eq. 5}$$

where the integral from time = 0 to t is obtained directly from the measured data. In the current study, the biological parameters (α_1, α_2, λ_1, λ_2) were obtained by fitting a two-component exponential to data from each organ as described above. Equation 5 was used to calculate τ/V after the measurement period for all source organs other than bladder contents. Residence time per unit volume was multiplied by the organ volumes defined for the MIRD anthropomorphic phantom (*23*) to give the residence time for each source organ. Equation 1 was used to calculate the mean dose to each target organ for which S values are tabulated, from all the source organs for which τ could be specifically measured.

The residence time for the *remainder of the body* was calculated as the total residence time for the entire body minus the specific residence times for the individually measured source organs. The S value for dose to each individual target organ from the remainder of the body source was calculated as described previously (*25–27*).

MIRD Pamphlet No. 14 Calculations

In the general MIRD anthropomorphic model, the urinary bladder has fixed size, volume and position (*23*). The limitations of this model are well recognized. Several major efforts have been directed at creating a more realistic bladder model that retained the applicability and ease of use of the general MIRD schema (*19,28–33*). In *MIRD Pamphlet No. 14* (*7*) these methods were reviewed, and a bladder model was proposed that retained the major features of the previously described dynamic urinary models, while keeping estimates and calculations as simple as possible. This pamphlet, as originally published, contains errors in Equations 2 and 3 (corresponding to Eqs. 6 and 7 of this article) and in the tabulated results derived therefrom; an erratum subsequently was published (*34*).

In the *MIRD Pamphlet No. 14* model the bladder is considered to be spherical, an approximation whose acceptability has been documented (*19*). The volume of urine entering the bladder is constant during the day. *MIRD Pamphlet No. 14* tabulations correspond to three discrete urine production rates. A fixed postvoid residual bladder volume of 10 ml is used. The volume of bladder contents at the time of injection is variable from 10–500 ml. Injection time is assumed to be 9 am. The time of the first void is variable from 20 min to 3 hr after tracer injection. Thereafter, a fixed void schedule is assumed, modified for an overnight gap. Excretion of tracer into the bladder is described by a sum of biological exponential components. Bladder contents activity as a function of time is given by:

$$A(t) = A_0\, e^{-\lambda t} \sum_{j=1}^{m} \alpha_j (1 - e^{-\lambda_j t})$$

$$- \sum_{i=1}^{n} \left(1 - \frac{V_r}{V(T_i)}\right) A(T_i) e^{-\lambda(t-T_i)} \qquad \text{Eq. 6}$$

where:

λ is the physical decay time constant,
α_j and λ_j are the intercept and time constant, respectively, of the j^{th} renal excretion term,
T_i is the time of the i^{th} void, and
V_r is the postvoid residual volume.

The first term describes input to the bladder contents by renal excretion; the second term represents the sum of all voids. Both are corrected for physical decay. The bladder wall surface dose rate from activity in the bladder contents is derived by Chen et al. (*19*). Removing unit-specific constants, the mean radiation absorbed dose $\bar{D}$ to the bladder wall surface is given by:

$$\bar{D} = \int_0^{\infty} \left[\frac{3.89\Gamma' A(t)}{V(t)^{2/3}} + \frac{\Delta_\beta A(t)}{2\rho V(t)}\right] dt \qquad \text{Eq. 7}$$

where:

3.89 is an approximation of a geometrically-derived constant $3\sqrt{6\Pi^2}$,

Γ' is the gamma ray exposure rate constant (converted from exposure to absorbed dose), whose value for ^{18}F as used in *MIRD Pamphlet No. 14* is 4.13×10^{-4} mGy · cm^2/MBq · s,

Δ_β is the mean electron particle energy emitted per nuclear transition, whose value for ^{18}F as used in *MIRD Pamphlet No. 14* is 4.00×10^{-8} Gy · kg/MBq · s,

ρ is the physical density of the bladder contents, for which a value of 1 is assumed, and

A(t) and V(t) are bladder contents activity and volume, as functions of time.

The first term corresponds to gamma dose and the second term to electron (positron) dose.

For these calculations, a spreadsheet was created in which values of activity, volume, residence time and dose were generated for every minute after injection. Given the rate of change of bladder contents activity, the use of 1-min time segments is adequate for accurate numerical integration. Since it was designed to calculate dosimetry for individual subjects with measured urinary excretion parameters, this spreadsheet allows the user to enter actual values for certain parameters that have fixed or discrete values in the *MIRD Pamphlet No. 14* formulation such as urine production rate, postvoid residual volume and injection time. After the first void, the *MIRD Pamphlet No. 14* assumptions regarding the subsequent voiding schedule were used. The dose to the bladder wall surface and the residence time of activity within the bladder were calculated to 9 am the following day, by which time the activity remaining in the body was so small that the final void changed the total absorbed dose on the order of 0.1%.

MIRD Pamphlet No. 14 Modified to Use Measured Bladder Contents Data to First Void

Because calibrated time-activity curves for bladder contents were available for each subject, these data were used explicitly by modifying the *MIRD Pamphlet No. 14* method: the measured time-activity curve for each subject before first void was substituted for that portion of the *MIRD Pamphlet No. 14* calculated time-activity curve. Using Equation 7, the dose rate to the bladder wall was calculated for each 1-min time segment. These were numerically integrated to give the individual's bladder wall dose to the time of first void. The measured time-activity curve was integrated to provide the actual residence time of activity in the bladder contents to the first void. Residence time and bladder wall dose values from the time of first void to 9 am the next day were then calculated using *MIRD Pamphlet No. 14* methods as described above.

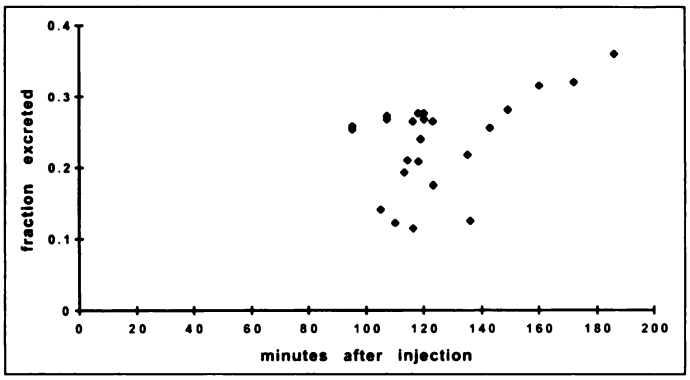

FIGURE 1. Fraction of administered nuclide excreted into urine (decay corrected) as function of void time; 24 measurements from 18 subjects.

Effective Dose

In the ICRP *Recommendations* adopted in November of 1990 (*20*), the *effective dose* E replaces the *effective dose equivalent* H_E (*35*). The effective dose is a means of providing a single number that represents the probability of stochastic biological effects due to an exposure to radiation, taking into consideration the variable radiosensitivity of body tissues; it consists of a weighted mean of doses to the various tissues. Units for effective dose are Sv (SI) and rem (traditional). The effective dose calculations for this article were performed under the assumption that doses to organs other than specifically calculated target organs are equal to the mean total body dose.

RESULTS

In 18 subjects, complete urine collections were obtained at the end of the scanning procedure, 95–135 min after injection. In 6 of these subjects, a subsequent complete void collection was obtained between 135 min and 3 hr after injection. In each case, the total volume and activity of voided urine was measured and corrected for decay to the time of injection, then divided by the administered dose to yield the fraction of tracer excreted into the urine to that time. These data are presented in Figure 1. The amount of administered radionuclide that is recovered in the urine at 2 hr is approximately 23% and at 3 hr is approximately 31%.

Least-squares fitting of a two-component exponential function to the mean body tissues retention curve from these subjects yielded:

$$A(t) = A_0(0.819e^{-0.000607t} + 0.178e^{-0.0286t}) \qquad \text{Eq. 8}$$

where time is in minutes and the time constants in minutes^{-1}. These coefficients and time constants were used for calculations of total body and bladder contents activities. A typical bladder curve and corresponding body retention curve are presented in Figure 2; the latter is graphed with the curve represented by the above equation for comparison.

Absorbed doses to the bladder wall surface were calculated using bladder contents only as the source and using all source organs; the general MIRD methodology was used to calculate the component of bladder wall dose from sources other than the bladder contents. Table 1 presents these results using each of the three methods of calculating bladder wall dose from bladder contents described above: *MIRD Pamphlet No. 14* methodol-

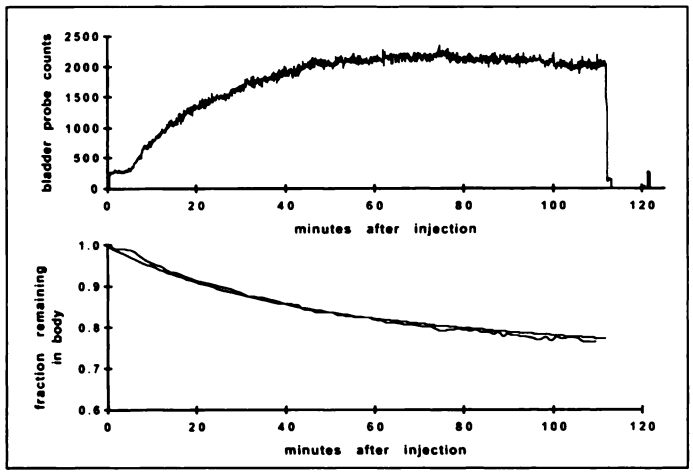

FIGURE 2. (A) Representative time-counts curve for bladder contents. Lower activity briefly measured at about 112 min is background activity. Peak after 120 min is measurement of postvoid residual activity. (B) Corresponding body tissues retention curve for this subject. Mean population body retention curve (smooth line) is graphed with this for comparison.

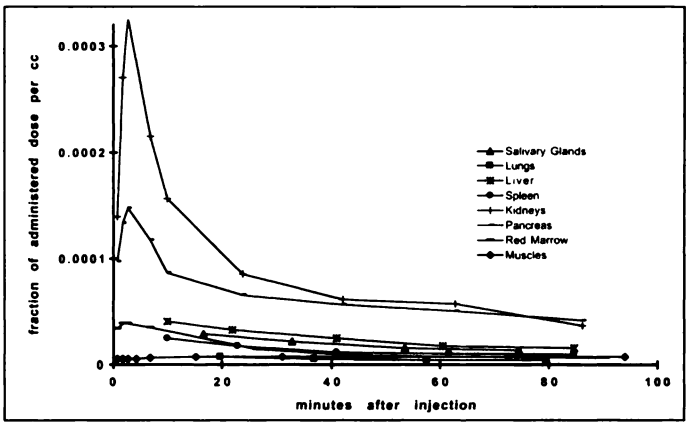

FIGURE 3. Fractional activity versus time for major source organs. Renal activity is relatively high because of urinary excretion of tracer. Pancreas is the other organ with tracer accumulation significantly greater than mean.

ogy; *MIRD Pamphlet No. 14* methodology modified to use the measure time-activity curve for bladder contents before the first void and general MIRD methodology using the static bladder model as described in *MIRD Pamphlet No. 5, Revised.* The general MIRD results, presented for comparison with older published dosimetry, are calculated from the mean bladder contents residence time of 15.63 min.

Because of the short physical half-life of ^{18}F, a large portion of bladder wall dose is received before the first void. Based on the modified *MIRD Pamphlet No. 14* calculations, the bladder wall surface dose from activity in the bladder contents reached an average of 68% of its total before first void at an average time of 115 min after injection.

In the rectilinear whole-body scans, no specific accumulation was identifiable in any major organ. The whole-body dynamic PET scans provided activity time courses for the organs presented in Figure 3. Since no specific tracer accumulation could be identified in the adrenal glands, the gastrointestinal tract, the gonads or the thyroid gland, these organs were considered for the purposes of these dosimetry calculations to be part of the remainder of the body source. Activity time courses for brain ROIs and for blood are presented in Figures 4 and 5.

Table 2 lists values of residence time per unit volume for the blood and for all organs whose activity time courses were measured by PET, calculated using Equation 5; where the volume of the organ is defined for the MIRD phantom, total organ residence time also is given. The residence time values for the bladder contents are derived from the calculations described previously. These data show residence time per volume in the striata (caudates and putamina) that are an order of magnitude above those for organs without specific uptake, whereas the brain as a whole is comparable to abdominal organs.

The values for absorbed dose in Table 3 for organs other than bladder wall were obtained using the residence time (τ) values from Table 2 (converted to hours) and published values for S (*24*). Table 3 includes corresponding organ absorbed dose values from previously published dosimetry for direct comparison.

Using the specific target organ doses presented here, plus the assumption that doses for other organs are equal to the mean total body radiation dose, the effective dose per unit administered dose is 0.0199 mSv/MBq (0.0735 rem/mCi).

DISCUSSION

In this article, we present data and calculations indicating a mean bladder wall surface absorbed dose per unit administered activity of 0.150 mGy/MBq and an effective dose of 0.0199 mSv/MBq. Previous articles estimating fluoro-DOPA dosimetry (*1,8,9,36*) have reported bladder wall dose values from 0.15–0.695 mGy/MBq; the values presented for effective dose equivalent are from 0.0176–0.0539 mSv/MBq. These widely varying results are due to differences in how this tracer was used, how the measurements were made, and which calculation methods were used, all of which have evolved over time.

The data in the current article that are most directly comparable to those from the earliest article of fluoro-DOPA dosimetry (*1*) are the determinations of percentage of administered tracer that is recovered in the urine. There is a significant decrease from the previously reported values of 40% at 2 hr and

TABLE 1
Absorbed Dose at Bladder Wall Surface

	From bladder contents (mGy/MBq)	(rad/mCi)	From all sources (mGy/MBq	(rad/mCi)
*MIRD Pamphlet No. 14**	0.144	0.534	0.153	0.565
MIRD Pamphlet No. 14, modified†	0.142	0.525	0.150	0.556
General MIRD schema	0.127	0.470	0.136	0.501

*Method differs from that in *MIRD Pamphlet No. 14* only in the use of actual injection times, postvoid volumes and urine production rates instead of fixed or discrete assumptions.

†Measured time-activity curves for bladder contents were used in place of the calculated bladder contents curves up to the first void. Actual injection times, postvoid volumes and urine production rates were used as above.

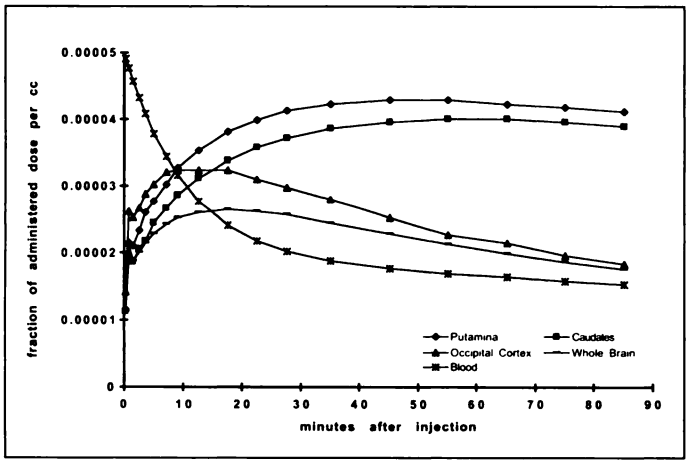

FIGURE 4. Mean fractional activity versus time for brain regions. Fractional activity of whole blood is shown for comparison.

48% at 3 hr to the values reported here of 23% and 31%, respectively. This change is apparently attributable to the preadministration of carbidopa. It is well known that carbidopa markedly alters the absolute and relative amounts of major metabolites in the plasma (*3–6*). These different chemical forms would be expected to have different renal excretion rates and, therefore, have a significant effect on bladder dosimetry; absorbed dose values and biodistribution data obtained in situations in which carbidopa was not administered according to current practices (*1,8*) should, therefore, be replaced.

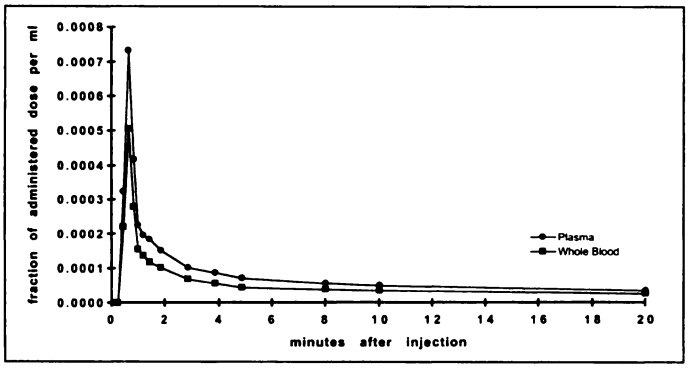

FIGURE 5. Whole blood and plasma fractional activity versus time during first 20 min after tracer injection. During this period, plasma activity is significantly greater than that of whole blood. These values are nearly identical by 90 min.

TABLE 2
Residence Times

Organ	τ/V(min/cm^3)	τ(min)*
Bladder contents	—	15.63
Whole blood	0.00238	—
Caudate nucleus	0.0495	—
Putamen	0.0311	—
Occipital cortex	0.00431	—
Whole brain	0.00452	6.64
Kidneys	0.00743	2.14
Liver	0.00284	5.20
Lungs	0.00077	2.61
Muscle	0.00104	29.46
Pancreas	0.00624	0.38
Red marrow	0.00144	2.19
Salivary glands	0.00255	—
Spleen	0.00183	0.32
Remainder of body†	—	74.54

*Given for organs whose volumes are defined in the MIRD anthropomorphic phantom (*23*) and for bladder contents and remainder of body (derived directly as described in the text).

†Body tissues minus kidneys, liver, lungs, muscle, pancreas, red marrow and spleen.

TABLE 3
Absorbed Doses to Target Organs

	Mean absorbed dose		Comparison from Harvey (*1*)	Comparison from Mejia (*8*)
Organ/structure	(mGy/MBq)	(rad/mCi)	(mGy/MBq)	(mGy/MBq)
Adrenals	0.0150	0.0555	—	0.014
Bladder wall*	0.150	0.556	0.695	0.215
Bone (total)	0.0107	0.0397	0.0070	0.010
Stomach wall	0.0121	0.0447	0.0073	0.010
Small intestine wall	0.0141	0.0523	0.0114	0.012
Upper large intestine wall	0.0140	0.0516	0.0111	0.011
Lower large intestine wall	0.0160	0.0593	0.0187	0.014
Kidneys	0.0274	0.101	0.0074	0.089
Liver	0.0154	0.0570	0.0087	0.008
Lungs	0.0127	0.0471	0.0063	0.004
Red marrow	0.0105	0.0390	0.0085	0.013
Other tissues (muscle)	0.0089	0.0331	0.0088	0.006
Ovaries	0.0141	0.0521	0.0167	0.013
Pancreas	0.0197	0.0728	0.0072	0.030
Skin	0.0085	0.0314	0.0057	—
Spleen	0.0117	0.0431	0.0084	0.009
Testes	0.0148	0.0548	0.0152	0.015
Thyroid	0.0103	0.0379	0.0059	0.007
Uterus	0.0186	0.0688	0.0307	0.020
Total body	0.0105	0.0388	0.0090	—

**MIRD Pamphlet No. 14*, modified, result from Table 1.

Two prior articles of fluoro-DOPA biodistribution have been based on data from dogs (*1*) and mice (*8*). Differences between the human and animal data appear to be due to a combination of species differences and the use of carbidopa. For instance, liver and spleen activity in our data are not significantly higher than in other organs. Both of these organs were identified as having higher tracer accumulation in the dog, and liver accumulation was similarly high in the mouse. Carbidopa, which affects hepatic metabolism of the tracer, was not used in the animal studies. The pancreas, on the other hand, was identified as an organ with higher tracer accumulation in our human data and in mice, but not in dogs. Apparently, this difference is a species effect unrelated to carbidopa.

Two measurement methods used in our studies have allowed the detailed collection of human data. The use of an external bladder probe, along with complete voided urine collection, to provide a calibrated time-activity curve for bladder contents is similar to the methods used by Jones et al. (*37*) in 1982 for evaluating fluorodeoxyglucose bladder dosimetry and Mejia et al. (*8*) for fluoro-DOPA and other tracers. This method makes it unnecessary to use conservative, unrealistic estimates of bladder contents activity. The second methodological change in data acquisition presented here is the use of dynamic whole-body quantitative PET scanning for deriving time-activity curves for multiple organs. Dynamic PET has been applied by Dhawan et al. (*9*) in the pelvis for generating bladder contents time-activity curves and by Mejia et al. (*8*) for generating whole brain time-activity curves. PET measurements were used in the current study in such a way as to include all tissues from the base of the head through the upper thigh for the measurement of time-activity curves for multiple organs in a single subject.

Previous articles have used the static bladder model of the ICRP (*1,38*) and the MIRD Committee (*8–9*). Even the publication describing the anthropomorphic MIRD phantom warns against over-interpreting the accuracy of the fixed-volume bladder model (*23*). Thus, the work culminating in *MIRD Pamphlet No. 14* (*7*) is an important amendment. The short physical half-life of most of the radionuclides used in PET, plus the beta dose from the positrons that penetrate only a short distance, accentuate the importance of a more detailed and physiologically accurate bladder model. In particular, the bladder wall surface absorbed dose calculation derived by Chen et al. (*19* and Eq. 7) points out the critical dependence of absorbed dose on bladder contents volume, especially at small volumes. While the data in the current article show a fairly modest difference between the calculated bladder wall absorbed dose using the general MIRD phantom versus the *MIRD Pamphlet No. 14* methods, this is heavily dependent on the particular bladder volumes and urine production rates represented in this study protocol and, therefore, cannot be interpreted uncritically. The relatively long time taken in the present studies to position the subject and to obtain a transmission scan before tracer injection have a major effect on the volume of bladder contents at the time of tracer injection, which is one of the most significant determinants of bladder wall radiation dose. In addition, because of the short physical half-life, as well as the decreasing biological entry of tracer into the bladder after the first hour, the time from tracer injection to first void is important.

Many of the conventions and simplifications used in the *MIRD Pamphlet No. 14* methods are designed to provide straightforward methods for predicting dosimetry from a given radiopharmaceutical under specific conditions and, as such, are tailored for the uses described in the preceding paragraph. Certain modifications to the *MIRD Pamphlet No. 14* methods have been made in the present article such that the calculated dosimetry values for individual subjects are based directly on urine data measured from those subjects. These modifications represent a replacement of *MIRD Pamphlet No. 14* simplifications with explicitly measured information, without any change in the physiologic bladder model or the calculation of bladder wall surface dose from bladder contents. Thus, the results presented here accurately reflect the urinary physiology of our subjects under our specific study conditions. Our protocol did not include manipulations specifically aimed at decreasing bladder wall dose, such as subject hydration or early void times (*9,12*); rather, it reflects conditions for a typical brain PET scan, consisting of a transmission scan followed by a lengthy dynamic emission scan.

CONCLUSION

The human data presented here indicate that carbidopa pretreatment has a significant effect on fluoro-DOPA biodistribution and dosimetry. This phenomenon would not be expected to be unique to carbidopa. Any experimental manipulation that changes the amount or nature of labeled metabolites should be assumed to cause changes in biodistribution and dosimetry. It also is apparent from these data that more than two-thirds of the bladder wall absorbed dose is typically received before the first void; tailoring the experiment to minimize absorbed dose before first void will, therefore, be of the greatest importance in minimizing subject dose. Since bladder wall dose is a complex function of bladder contents volume and activity (*7,19*), a physiological bladder model should be used in planning scan protocols.

ACKNOWLEDGMENTS

This work was funded in part by National Institute of Neurological Diseases and Stroke Grant No. R29 NS31612 and by NIH NRSA Training Grant No. CA09206.

REFERENCES

1. Harvey J, Firnau G, Garnett ES. Estimation of the radiation dose in man due to 6-[^{18}F]fluoro-L-dopa. *J Nucl Med* 1985;26:931–935.
2. Garnett ES, Firnau G, Nahmias C. Dopamine visualized in the basal ganglia of living man. *Nature* 1983;305:137–138.
3. Boyes BE, Cumming P, Martin WR, McGeer EG. Determination of plasma [^{18}F]-6-fluorodopa during positron emission tomography: elimination and metabolism in carbidopa treated subjects. *Life Sci* 1986;39:2243–2252.
4. Firnau G, Sood S, Chirakal R, Nahmias C, Garnett ES. Metabolites of 6-[^{18}F]fluoro-L-dopa in human blood. *J Nucl Med* 1988;29:363–369.
5. Melega WP, Hoffman JM, Luxen A, Nissenson CHK, Phelps ME, Barrio JR. The effects of carbidopa on the metabolism of 6-[^{18}F]fluoro-L-DOPA in rats, monkeys and humans. *Life Sci* 1990;47:149–157.
6. Hoffman JM, Melega WP, Hawk TC, et al. The effects of carbidopa administration on 6-[^{18}F]fluoro-L-dopa kinetics in positron emission tomography. *J Nucl Med* 1992;33: 1472–1477.
7. Thomas SR, Stabin MG, Chen C-T, Samaratunga RC. MIRD Pamphlet No. 14: a dynamic urinary bladder model for radiation dose calculations. *J Nucl Med* 1992;33: 783–802.
8. Mejia AA, Nakamura T, Itoh M, et al. Absorbed dose estimates in positron emission tomography studies based on the administration of ^{18}F-labeled radiopharmaceuticals. *J Radiat Res (Tokyo)* 1991;32:243–261.
9. Dhawan V, Belakhlef A, Robeson W, et al. Bladder wall radiation dose in humans from fluorine-18-FDOPA. *J Nucl Med* 1996;37:1850–1852.
10. Oakes, TR. Dosimetry of ^{18}F-DOPA in humans. In: Oakes, TR. *Clinical investigation of the dopaminergic system with PET and 18F-fluoro-L-DOPA* [Doctoral Thesis]. Madison, WI: University of Wisconsin;1995:72–84.
11. Brown WD, Oakes TR, Nickles RJ. Revised dosimetry for fluoro-DOPA with carbidopa pretreatment. *J Nucl Med* 1993;34:157P.
12. Lu E, Meyer E, Kuwabara H, Ma Y, Shiraishi M, Evans AC. Reduction of radiation absorbed dose in ^{18}F FDOPA PET studies by hydration-induced voiding. *J Nucl Med* 1995;36(suppl):98P.
13. Roberts AD, Oakes TR, Nickles RJ. Development of an improved target for [^{18}F]F_2 production. *Appl Radiat Isot* 1995;46:87.
14. Namavari M, Bishop A, Satyamurthy N, Bida G, Barrio JR. Regioselective radiofluorodestannylation with [^{18}F]F_2 and [^{18}F]CH_3COOF: a high yield synthesis of 6-[^{18}F]fluoro-L-DOPA. *Int J Radiat Instrum Part A* 1990;41:275–281.
15. Rinne UK, Laihinen A, Rinne JO, Nagren K, Bergman J, Ruotsalainen U. Positron emission tomography demonstrates dopamine D_2 receptor supersensitivity in the striatum of patients with early Parkinson's disease. *Movement Disorders* 1990;5:55–59.
16. Antonini A, Vontobel P, Psylla M, et al. Complementary positron emission tomographic studies of the striatal dopaminergic system in Parkinson's disease. *Arch Neurol* 1995;52:1183–1190.
17. Brooks DJ, Salmon EP, Mathias CJ, et al. The relationship between locomotor disability, autonomic dysfunction, and the integrity of the striatal dopaminergic system in patients with multiple system atrophy, pure autonomic failure, and Parkinson's disease, studied with PET. *Brain* 1990;113:1539–1552.
18. Eidelberg D, Moeller JR, Dhawan V, et al. The metabolic anatomy of Parkinson's disease: complementary [^{18}F]fluorodeoxyglucose and [^{18}F]fluorodopa positron emission tomographic studies. *Movement Disorders* 1990;5:203–213.
19. Chen C-T, Harper PV, Lathrop KA. A simple dynamic model for calculating radiation absorbed dose to the bladder wall. In: *4th International Radiopharmaceutical Dosimetry Symposium, Nov 5–8, 1985*. CONF-851113-(DE86010102). Oak Ridge, TN: Oak Ridge National Laboratories; 1985:587–612.
20. International Commission on Radiological Protection. ICRP Publication 60: 1990 Recommendations of the International Commission on Radiological Protection. *Annals of the ICRP* 1991;21(1–3).
21. Brooks DJ, Ibanez V, Sawle GV, et al. Differing patterns of striatal ^{18}F-dopa uptake in Parkinson's disease, multiple system atrophy, and progressive supranuclear palsy. *Ann Neurol* 1990;28:547–555.
22. Loevinger R, Berman M. *MIRD pamphlet no. 1, revised: a revised schema for calculating the absorbed dose from biologically distributed radionuclides*. New York: Society of Nuclear Medicine;1976.
23. Snyder WS, Ford MR, Warner GG. *MIRD pamphlet no. 5, revised: estimates of specific absorbed fractions for photon sources uniformly distributed in various organs of a heterogeneous phantom*. New York: Society of Nuclear Medicine;1978.
24. Snyder WS, Ford MR, Warner GG, Watson SB. *MIRD pamphlet no. 11: "S," absorbed dose per unit cumulated activity for selected radionuclides and organs*. New York: Society of Nuclear Medicine;1975.
25. Loevinger R, Budinger TF, Watson EE. *MIRD primer for absorbed dose calculations*, revised edition. New York: Society of Nuclear Medicine;1991.
26. Snyder WS, Ford MR, Warner GG, Watson SB. *A tabulation of dose equivalent per microcurie-day for source and target organs of an adult for various radionuclides*. ORNL-5000. Oak Ridge, TN: Oak Ridge National Laboratory;1975:16–19.
27. Coffey JL, Watson EE. Calculating dose from remaining body activity: a comparison of two methods. *Med Phys* 1979;6:307–308.
28. Snyder WS, Ford MR. Estimation of dose to the urinary bladder and to the gonads. In: *Radiopharmaceutical dosimetry symposium*. Oak Ridge, TN: Oak Ridge National Laboratories; 1976:313–350.
29. Smith EM, Warner GG. Practical methods of dose reduction to the bladder wall. In: *Radiopharmaceutical dosimetry symposium*. Oak Ridge, TN: Oak Ridge National Laboratories; 1976:351–359.

30. Diffey B, Hilson A. Absorbed dose to the bladder from 99mTc-DTPA [Letter]. *Brit J Radiol* 1976;49:196–198.
31. Unnikrishnan K. Dose to the urinary bladder from radionuclides in urine. *Phys Med Biol* 1974;19:329–340.
32. Smith T, Veall N, Wotton R. Bladder wall dose from administered radiopharmaceuticals: the effects of variations in urine flow rate, voiding interval, and initial bladder content. *Radiat Prot Dosim* 1982;2:183–189.
33. Chen C-T, Harper PV, Lathrop KA. Radiation absorbed dose to the bladder from 2-FDG and other radiopharmaceuticals. *J Nucl Med* 1984;25:92–93.
34. The MIRD Committee erratum. *J Nucl Med* 1994;35:73.
35. International Commission on Radiological Protection. *ICRP publication 26: recommendations of the International Commission on Radiological Protection*. New York: Pergamon Press;1977.
36. Huda W, Sandison GA. Estimates of the effective dose equivalent, H_E, in positron emission tomography studies. *Eur J Nucl Med* 1990;17:116–120.
37. Jones SC, Alavi A, Christman D, Montanez I, Wolf AP, Reivich M. The radiation dosimetry of 2-[F-18]fluoro-2-deoxy-D-glucose in man. *J Nucl Med* 1982;23:613–617.
38. International Commission on Radiological Protection. *ICRP publication 30: limits for intakes of radionuclides by workers*. New York: Pergamon Press;1979.

(Continued from page 5A)

FIRST IMPRESSIONS
Technetium-99m-HMPAO White Blood Cell (WBC) Imaging of Widespread Myositis

Figure 1.

PURPOSE
A 24-yr-old previously healthy man presented with flu-like illness and a 10-day history of fever, severe bilateral thigh pain, diarrhea, vomiting, chest pain and an episode of hemoptysis. The patient was a cigarette smoker, methaqualone and cannabis abuser and an alcoholic. He was referred to a secondary hospital and found to have bilateral infiltrates on chest radiography. The patient was then treated with intravenous cefuroxime, erythromycin and gentamycin and was given inotropic support, but his condition deteriorated and he was admitted to our hospital in a state of septicemic shock. Laboratory investigations showed leukocytosis, raised serum urea and creatinine and very high levels of creatine phosphokinase (14,490 U/liter). The tracheal aspirate yielded a mixed growth of organisms on culture, but blood cultures were persistently negative. Provisional diagnoses of bronchopneumonia and myositis were made. The patient did not respond to the initial treatment and was referred for a ^{99m}Tc-hexamethyl propyleneamine oxime (HMPAO)-labeled WBC scan in an attempt to localize a source of infection. The scan showed extensive patchy tracer uptake involving most major skeletal muscle groups, especially in the limbs (Fig. 1). Abnormal uptake in the left chest was partially due to the active pneumonic process in the left lung. Normal tracer activity in the liver, spleen and urinary bladder was also seen. Radioactive urine in the extension tubing of the urinary catheter can be outlined (arrow). The patient responded to treatment with intravenous vancomycin, ciproflox and flucloxacillin and was discharged after 2 wk.

TRACER
Technetium-99m-HMPAO-labeled WBC (800 MBq)

ROUTE OF ADMINISTRATION
Intravenous

TIME AFTER INJECTION
18 hr

INSTRUMENTATION
Elscint Apex 409 ECT (Haifa, Israel) gamma camera with low-energy, all-purpose collimator

CONTRIBUTORS
Mohammad A.F. Nizami, MD, and Bruce K. Adams, MD, Department of Nuclear Medicine, University of Cape Town and Groote Schuur Hospital, Cape Town, South Africa